Journal of Medicinal Chemistry

ARTICLE

pubs.acs.org/jmc

Crystal Structure of *tert*-Butyldimethylsilyl-spiroaminooxathioledioxide-thymine (TSAO-T) in Complex with HIV-1 Reverse Transcriptase (RT) Redefines the Elastic Limits of the Non-nucleoside Inhibitor-Binding Pocket†

Kalyan Das,*[,‡,§] Joseph D. Bauman,[‡,§] Angela S. Rim,[‡,§] Chhaya Dharia,[‡,§] Arthur D. Clark, Jr.,[‡,§] María-José Camarasa,[∥] Jan Balzarini,[⊥] and Eddy Arnold*[,‡,§]

[‡]Center for Advanced Biotechnology and Medicine (CABM), [§]Department of Chemistry and Chemical Biology, Rutgers University, 679 Hoes Lane, Piscataway, New Jersey 08854, United States

[∥]Instituto de Química Médica (CSIC), Juan de la Cierva 3, 28006 Madrid, Spain

[⊥]Rega Institute for Medical Research, Katholieke Universiteit Leuven, B-3000 Leuven, Belgium

ABSTRACT: *tert*-Butyldimethylsilyl-spiroaminooxathioledioxide (TSAO) compounds have an embedded thymidine-analogue backbone; however, TSAO compounds invoke non-nucleoside RT inhibitor (NNRTI) resistance mutations. Our crystal structure of RT:7 (TSAO-T) complex shows that 7 binds inside the NNRTI-binding pocket, assuming a "dragon" shape, and interacts extensively with almost all the pocket residues. The structure also explains the structure−activity relationships and resistance data for TSAO compounds. The binding of 7 causes hyper-expansion of the pocket and significant rearrangement of RT subdomains. This nonoptimal complex formation is apparently responsible (1) for the lower stability of a RT (p66/p51) dimer and (2) for the lower potency of 7 despite of its extensive interactions with RT. However, the HIV-1 RT:7 structure reveals novel design features such as (1) interactions with the conserved Tyr183 from the YMDD-motif and (2) a possible way for an NNRTI to reach the polymerase active site that may be exploited in designing new NNRTIs.

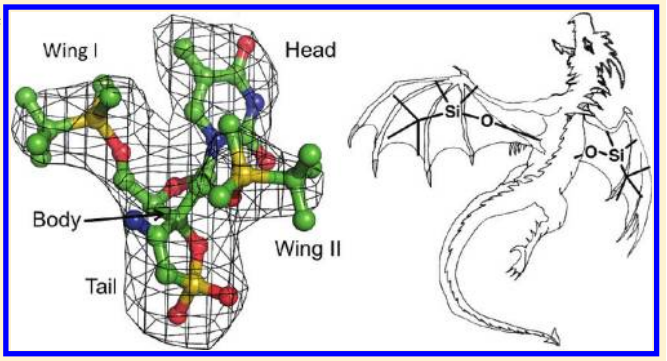

INTRODUCTION

In the life cycle of HIV-1, the viral enzyme reverse transcriptase (RT) copies the single-stranded viral RNA to a double-stranded (ds) DNA in the cytoplasm; the DNA is transported into the nucleus of the infected cell and integrated into the chromosome by another viral enzyme, HIV-1 integrase. Copying the viral RNA to dsDNA by RT involves the enzymatic steps of RNA-dependent DNA polymerization, RNase H cleavage of the RNA-strand from the RNA:DNA duplex, and DNA-dependent DNA polymerization. HIV-1 RT is a heterodimer of p66 (66 kDa) and p51 (51 kDa) subunits. The p66 subunit contains both the polymerase and RNase H active sites, whereas p51, the N-terminal proteolytically cleaved product of p66, plays a structural role. HIV-1 RT is targeted by almost half of the approved anti-AIDS drugs. RT is targeted by two classes of drugs: (1) the nucleoside/nucleotide RT inhibitors (NRTIs) that are incorporated into the growing DNA strand and block DNA polymerization, because all NRTI drugs lack 3′-OH and (2) the non-nucleoside RT inhibitors (NNRTIs)[1] that bind an allosteric site adjacent to the polymerase active site and restrict the structural flexibility of RT that is essential for carrying out DNA polymerization.

Diverse chemical classes of compounds have been found to bind the NNRTI-binding pocket (NNIBP), which is predominantly hydrophobic. In fact, the pocket does not exist in the structures of RT that are not bound to an NNRTI.[2−4] The shear movement of the β12−β13−β14 sheet with respect to the β6−β10−β9 sheet in the event of nucleotide incorporation and nucleic acid translocation is responsible for creating the NNIBP;[5] the β12−β13−β14 sheet contains the DNA-primer grip, and the β6−β10−β9 sheet contains the catalytic trio of aspartates (D110, D185, and D186) required for DNA polymerization. Once an NNRTI occupies the pocket between the two sheets, the DNA polymerization by RT is stalled. The NNRTIs **1** (nevirapine; 11-cyclopropyl-4-methyl-5,11-dihydro-6*H*-dipyrido[3,2-*b*:2′,3′-*e*][1,4]diazepin-6-one), **2** (delavirdine; *N*-[2-({4-[3-(propan-2-ylamino)pyridin-2-yl]piperazin-1-yl}carbonyl)-1*H*-indol-5-yl]methanesulfonamide), **3** (efavirenz; (4*S*))-6-chloro-4-(2-cyclopropylethynyl)-4-(trifluoromethyl)-2,4-dihydro-1*H*-3,1-benzoxazin-2-one), and **4** (etravirine; TMC125; 4-[6-amino-5-bromo-2-[(4-cyanophenyl)amino]pyrimidin-4-yl]oxy-3,5-di-

Received: December 1, 2010
Published: March 29, 2011

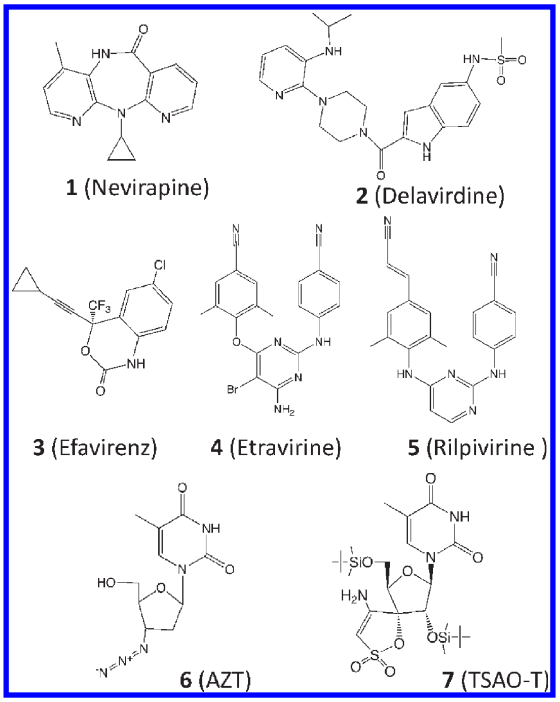

Figure 1. Chemical structures of NNRTI drugs **1** (nevirapine), **2** (delavirdine), **3** (efavirenz), **4** (etravirine), and **5** (rilpivirine), and the NRTI drug **6** (AZT; zidovudine) are compared with that of **7** (TSAO-T). The TSAO scaffold is distinct from other NNRTIs; however, it shares partial structural similarity with AZT.

methylbenzonitrile) are approved for treating HIV-1 infection. All NNRTIs occupy the NNIBP and mutations of the pocket amino acid residues confer NNRTI resistance; however, NNRTIs are chemically diverse, and different NNRTIs select different resistance mutations when used clinically. Also, an NNRTI-resistance mutation can result in negligible to severe resistance to an NNRTI, depending upon shape, size, and chemical composition of the NNRTI. The diarylpyrimidine (DAPY)[6] NNRTIs, **4** and **5** (rilpivirine; TMC278; 4-{[4-({4-[(*E*)-2-cyanovinyl]-2,6-dimethylphenyl}amino)pyrimidin-2-yl]-amino}benzonitrile),[7] have demonstrated broader efficacy against common NNRTI-resistance mutations because of their structural flexibility, permitting adaptation to changes in the NNIBP.[8,9] In general, more than two NNRTI-resistance mutations are required to cause noticeable resistance to these DAPY NNRTIs.[10] Accumulation of resistance mutations[11] and drug toxicity upon long-term use of anti-AIDS drugs remain as key concerns that motivate the discovery of new drugs, including new NNRTIs, to be effective against existing resistant mutant HIV-1 strains.

The TSAO ([2′,5′-bis-*O*-(*tert*-butyldimethylsilyl)-β-D-ribofuranosyl]-3′-spiro-5″-[4″-amino-1″,2″-oxathiole-2″,2″-dioxide]) class of inhibitors have been developed and characterized since the early 1990s.[12] A wide variety of TSAO analogues (modified at different positions, including the base, sugar, spiro, and *tert*-butyldimethylsilyl (TBDMS) groups) have been synthesized and investigated for their anti-HIV-1 activities; for an overview, see the review by Camarasa et al. 2004.[13] The TSAO backbone is distinctly different from other chemical classes of NNRTIs, and the most active derivatives partly share chemical structure resemblance with thymidine-analogue NRTIs (Figure 1). Some distinct features of TSAO[13−16] are: (1) the TSAO scaffold

Table 1. Anti-HIV-1 Activity of 7 (TSAO-T[14])/8 (TSAO-m^{3}T[14b]) against Mutant HIV-1 Strains in CEM Cell Cultures[18−20,38]

HIV-1 strain	EC_{50}[a] (μg/mL)
WT	0.03
L100I	0.07−0.21
K103N	0.23
V106A	1.9−3.7
N136A/Q/K	>50
E138K	>3
E138D	0.01
V179N	0.22
Y181C	2−6.5
Y181I	>10
Y188H	>3.3
Y188L	>10
G190E	>10

[a] 50% Effective concentration required to inhibit syncytia formation in HIV-1(III_B)-infected CEM cell cultures.

is significantly larger than all known classes of NNRTIs, (2) TSAO has an embedded thymidine-analogue nucleoside moiety, yet it does not compete with the nucleotide binding or NRTI incorporation into viral DNA,[17] (3) although TSAO derivatives consistently select for the Glu138Lys resistance mutation in HIV-1 RT, many other NNIBP pocket mutations also confer significant resistance to TSAO (Table 1),[18−20] (4) sizes and shapes of the binding pocket[21] revealed by available crystal structures do not accommodate TSAO, and (5) TSAO destabilizes the p66/p51 heterodimer,[16,22,23] whereas many other NNRTIs enhance the stability of the heterodimer.[24] Owing to these unique characteristics of TSAO, the structural characterization of the binding of TSAO to HIV-1 RT is challenging but essential for understanding of its antiviral properties.

Here we report the crystal structure of the HIV-1 RT:**7** (TSAO-T) complex at 2.6 Å resolution that reveals an unexpected expansion of the NNIBP and consequential significant rearrangements of RT subdomains upon binding of **7**. Also, the structure helps to resolve the longstanding ambiguity on the binding site of TSAO and explain the resistance profile of the TSAO class of inhibitors.

RESULTS

Structure of the HIV-1 RT:7 (TSAO-T) Complex. Several laboratories including ours were unsuccessful in determining the structure of an HIV-1 RT:TSAO complex. We also had problems with obtaining good quality diffraction from crystals of flexible inhibitors such as **5**,[9] which were overcome by a systematic crystal engineering approach. The RT constructs RT52A and RT69A,[4] obtained by crystal engineering, enabled us to obtain structures of RT:NNRTI complexes and of apo RT, respectively, at high resolution. Our recent attempt to crystallize the RT:**7** complex yielded diffraction quality crystals only with RT69A, in contrast to RT52A, that has been optimized for crystallizing RT:**5** and several other RT:NNRTI complexes. X-ray diffraction data were collected at 2.6 Å resolution from a crystal of the RT69A:**7** complex on a Rigaku R-Axis IV^{++} image plate system using an in-house Cu rotating anode X-ray source. The unit cell parameters of crystals of the RT69A:**7** complex (space group *C*2;

Table 2. X-Ray Diffraction Data and Structure Refinement Statistics

Protein Data Bank (PDB) accession code	3QO9
X-ray source	Rigaku R-Axis IV^{++}
wavelength (Å)	1.54178
space group; cell constants (a, b, c in Å and β in deg)	C2 (162.76, 72.59, 108.97 and 98.75)
resolution range (last shell) in Å	40−2.6 (2.64−2.60)
no. of unique reflections (number of observations)	37 564 (166,539)
completeness (last shell)	96.5 (97.8) %
R_{merge} (last shell)	0.100 (0.553)
average $I/\sigma(I)$ (last shell)	18.4 (2.0)
cutoff criteria	$I \leq -1.0\ \sigma(I)$
Refinement Statistics	
total no. of atoms (inhibitor/solvent atoms)	7988 (38/36)
resolution (Å)	40−2.6
no. of reflections (R_{free} set)	37 540 (1,514)
completeness (R_{free} set)	96.5 (3.9) %
R_{work}/R_{free}	0.244/0.286
Ramachandran statistics (% of residues in favored/disallowed regions)	99.8/0.0
Procheck G factor[52]	0.15
rms bond lengths (Å)	0.0085
rms bond angles (deg)	1.6

a = 162.76, b = 72.59, c = 108.97 Å, β = 98.75°; Table 2), in particular the β angle, resembled a typical RT52A:NNRTI complex ($C2$; a = 163, b = 73, c = 110 Å; β = 100°) rather than those of apo RT69A RT ($C2$; a = 164, b = 72, c = 109 Å; β = 104°), which suggested that the RT69A:**7** complex apparently was a RT:NNRTI complex. The structure was solved by molecular replacement using the RT52A:**5** complex[9] as the starting model and refined at 2.6 Å resolution (Table 2). The electron density maps, calculated after cycles of model building of protein atoms and refinement, unambiguously defined the conformation of **7** in the pocket (Figure 2a).

The structure revealed that the NNIBP is substantially expanded compared to that in all known RT:NNRTI structures. This hyperexpansion of the pocket also influenced the rearrangement of the RT subdomains. It appears that the unusual expansion of the NNRTI-binding site upon binding of **7** and its effect on RT conformation was primarily responsible for earlier unsuccessful crystallization results and potentially for the weak efficacy of TSAO derivatives against NNRTI-resistant mutants (Table 1), as discussed in detail below.

Binding of TSAO-T to HIV-1 RT. The crystal structure and existing resistance data (Figure 2, Table 1) confirm that the TSAO compounds are indeed NNRTIs. The molecule **7**[14] in the NNRTI-binding pocket assumes a large "butterfly" or, rather a "dragon" conformation in which the thymine base, the central ribose ring, and rear spiro moiety resemble the head, body, and tail parts, respectively; the two TBDMS moieties at the 2′- and 5′-positions span on either side as two wings of the dragon-shaped NNRTI. Because of the relatively large size of **7**, its interactions with RT are distinct from the interactions of a typical "butterfly" NNRTI,[25] such as **1**. All of the binding pocket residues interact with **7** (Figure 2b,c). The aromatic side chains of Tyr181 and Tyr188 are arranged in a different conformation compared to the commonly observed NNRTI-bound conformation in which both of the aromatic side chains are on one side, forming a wall of the hydrophobic pocket; however, the currently observed conformations of Tyr181 and Tyr188 were also seen when HEPT[26] and pyridinone[27] derivatives bind HIV-1 RT. The hydrophobic valley created by the rearrangement of the two aromatic side chains accommodates the 5′-TBDMS (wing I) part of **7**. The wing I moiety extends further to interact with Trp229, Pro95, Tyr183, and Glu138 (p51); the amino acid residues Tyr183 (part of the conserved YMDD motif) and Trp229 (a part of the primer grip) are highly conserved. The wing II portion (2′-TBDMS) extends toward the rear end of the $\beta12-\beta13-\beta14$ sheet and interacts with Phe227, Tyr318, His235, and Pro236. Chemical substitutions on wing I are highly deleterious for antiviral activity of TSAO,[13,16,28−30] whereas chemical modifications of the 2′-TBSMS (wing II) have relatively less impact on the activity[28] as discussed in Structure−Activity Relationships (SAR) of TSAO. The thymine "head" is positioned between the aromatic side chains of Tyr188 and Phe227, stacks with Phe227, and points toward the flexible loop (residues 214−224) outside the NNIBP (Figure 3). The ribose "body" and spiro "tail" rings are positioned over the $\beta6-\beta10-\beta9$ sheet. One of the sulfonyl oxygens of the oxathioledioxide group forms a hydrogen bond (H-bond) with the main chain amino group of Lys103 (N···O distance 3.1 Å), whereas the other S═O group is involved in a water-mediated interaction network with RT (Figure 2b). Most of the potent NNRTIs have a characteristic hydrogen bond with the main chain amino group of Lys101. This interaction appears to improve the binding affinity and help orient an NNRTI in NNIBP; both NNRTIs and NNIBP are highly hydrophobic. The relatively weak hydrogen bond and the water-mediated interactions of **7** with the region Lys101-Lys103 may not have an optimal contribution for the binding of **7** compared to contribution from the characteristic hydrogen bond between a potent NNRTI and Lys101.

Effects of NNRTI-Resistance Mutations. The TSAO compounds **7**[14] and **8**[14b] lose a large fraction of their inhibitory potential (>30- to 100-fold) against HIV-1 viruses carrying NNRTI-characteristic mutations (Table 1). A more modest decrease in antiviral activity (i.e., 7- to 20-fold) was noticed for mutant virus strains containing mutations at positions 100 or

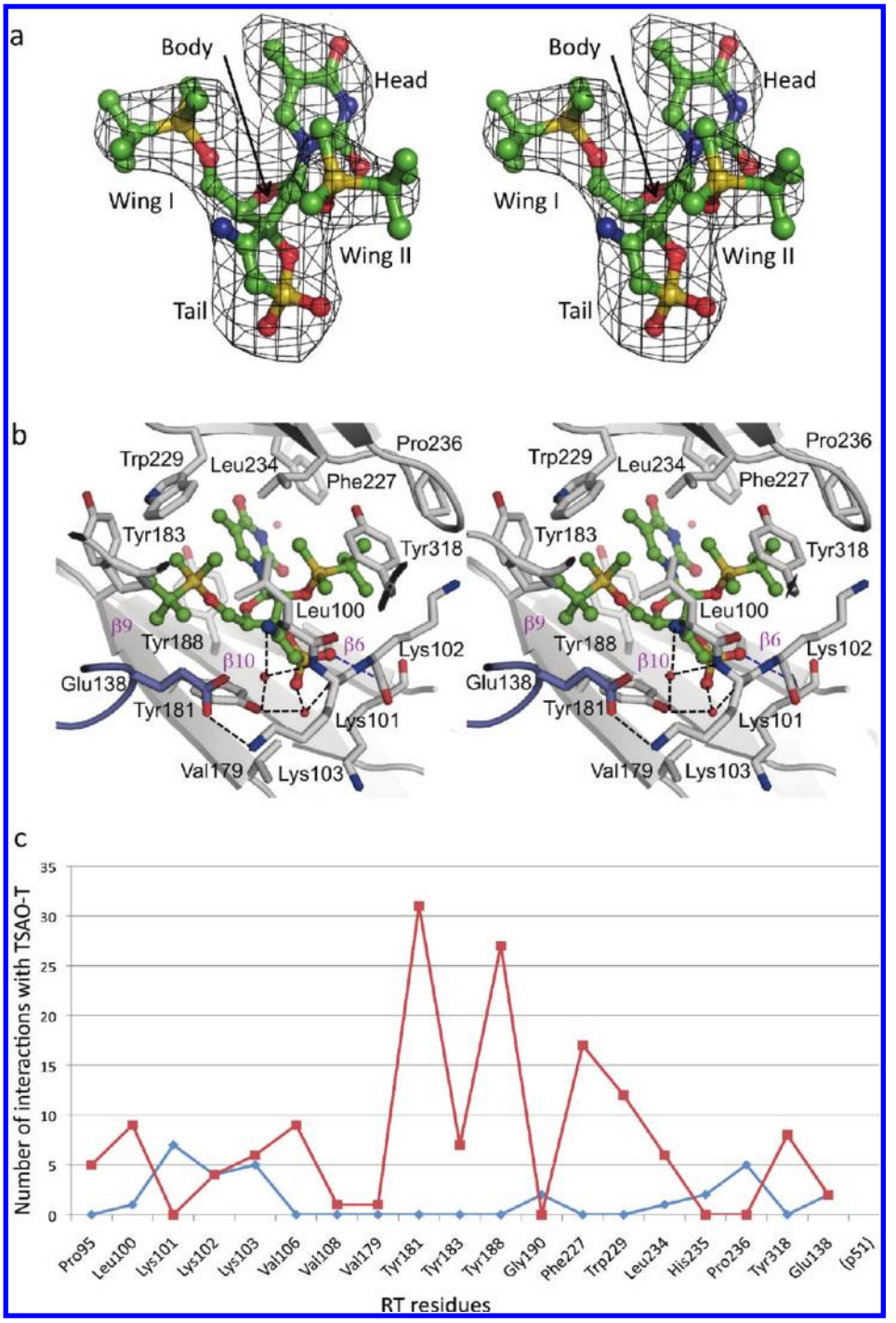

Figure 2. Binding of 7 (TSAO-T) to HIV-1 RT. Stereo views of: (a) difference ($|F_o| - |F_c|$) electron density enabled the unambiguous modeling of 7 in the binding pocket; the molecule 7 assumes a "dragon" shape; (b) the mode of binding of 7 (green) to HIV-1 RT (gray); the interacting amino acid residues and water molecules (red spheres) are shown. (c) Number of interactions (number of atom-to-atom distances ≤4.5 Å between 7 and RT residues) on the *y*-axis plotted against the respective RT amino acid residues on *x*-axis to assess the interactions of 7 with individual residues of RT. The red and blue lines correspond to the number of interactions of 7 with side chain and main chain atoms, respectively, of RT residues.

103. The TSAO compounds are the bulkiest known NNRTIs; the smallest in the series, 7 has a molecular weight of ∼590, and 7 has extensive interactions with the binding pocket residues (Figure 2b,c). In fact, 7 shares a maximum interacting surface area compared to any other NNRTI, including the potent DAPY NNRTIs; 7 has ∼735 Å^2 surface area, and a large portion of this surface interacts with the RT amino acid residues. Although the large inhibitor:protein interacting surface would be expected to markedly increase the binding affinity of the inhibitor, the binding affinity of 7 may be offset by the required hyperexpansion of the pocket. Also, the inability of 7 to wiggle and jiggle in the pocket,[9,31] because of its large size, explains why the antiviral

dx.doi.org/10.1021/jm101536x |*J. Med. Chem.* 2011, 54, 2727–2737

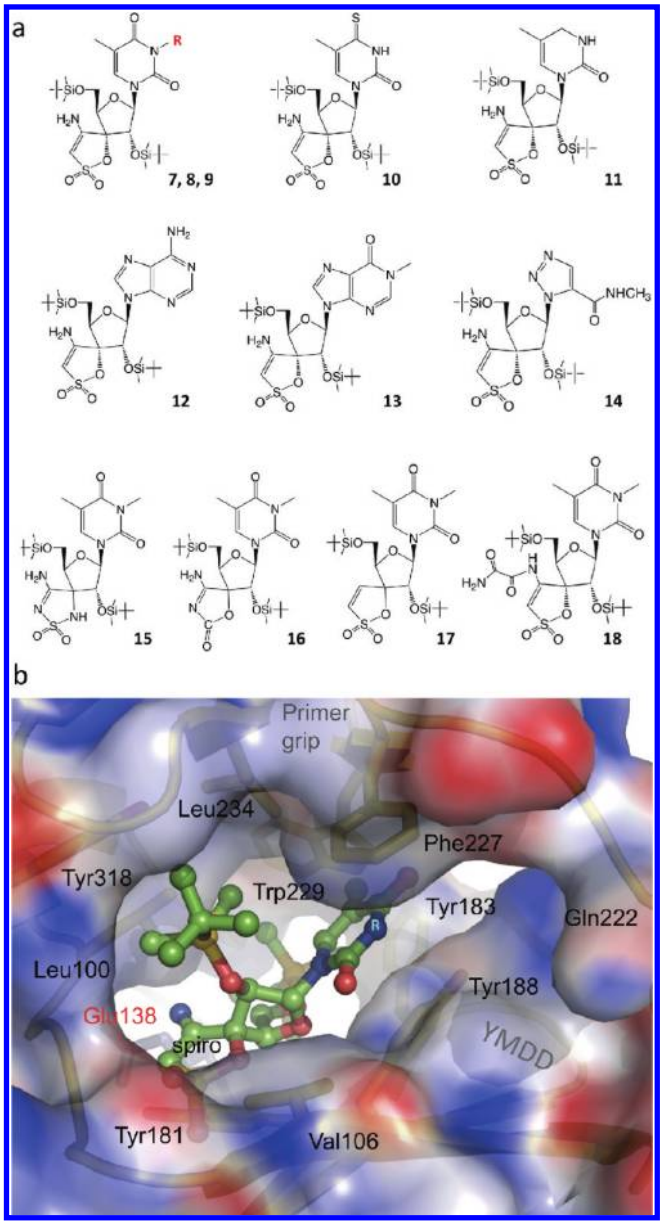

Figure 3. Structure−activity relationships (SAR) of TSAO. (a) Selected TSAO derivatives that were prepared and tested for HIV-1 inhibition (Table 4). The compounds were synthesized by the base substitutions with different R-groups and modifying the spiro moiety. Compounds **7** TSAO-T (R = H), **8** TSAO-m_3T (R = CH_3), and **9** (R = $(CH_2)_4$ $CONHCH_3$) are represented by the top left chemical structure. The compounds **7**−**14** have substituted or modified thymines, purines, or 1,2,3-triazole and the compounds **15**−**18** have modified spiro moieties. (b) Molecular surface of RT showing the binding of TSAO-T: the substituted R-group/purine/triazole ring would accommodate the large open space outside the pocket around a flexible loop (p66 residues 210−224). The spiro ring modifications are less tolerated except for the deletion of the amino group; the amino group has no significant interaction with RT.

activities of TSAO compounds are diminished in the presence of most common NNRTI-resistance mutations (Table 1). Mutations such as Tyr181Ile and Tyr188Leu/His maintain hydrophobicity yet cause high-level resistance to TSAO compounds by altering the shape of the pocket; **7** has maximum interactions with Tyr181 and Tyr188 compared to other amino acid residues (Figure 2c). The body and the tail of **7** reside over Val106 and Gly190, therefore, substitution of these two side chains (1) by a smaller side chain, such as Val106Ala, would lose some of the key inhibitor−protein interactions or (2) by larger side chains, such as Gly190Glu would cause steric hindrance. The mutations Leu100Ile and Val179Asn have relatively low impact on inhibition by TSAO compounds (Table 1). The Val179 side chain is located about 3.8 Å away from a terminal sulfonyl oxygen of the oxathiolane dioxide moiety of **7**; a mutated Asn179 side chain in the Val179Asn mutant RT would be pointing away from **7**. Similarly, a modeled Leu100Ile mutation does not appear to cause significant steric hindrance with **7**. Residue Lys103 has been proposed to be critical for the entry of most NNRTIs[3,32−35] even though the Lys103 side chain has little interaction with most NNRTIs. Apparently, binding of TSAO NNRTIs into NNIBP requires a significant rearrangement of the region including Glu138 of the p51 subunit.

The Glu138Lys Mutation and TSAO. Interestingly, Glu138Lys is a characteristic TSAO mutation that is invariably selected in cell culture upon exposure of HIV-1 to a variety of TSAO derivatives.[36,37] It causes a high degree of resistance to the TSAO derivatives (>100-fold). The structure revealed that the *tert*-butyl group of 5′-TBDMS arm has hydrophobic interactions with the main chain region of Glu138 of the p51 subunit. Therefore, a Glu138Lys mutation would not significantly alter these inhibitor:protein interactions. All substitutions at position 138 (Glu138Lys/Ala/Gln/Gly/Phe/Tyr), except Glu138Asp, which retains the effectiveness of TSAO, alter the charge environment of Glu138 and develop resistance to TSAO compounds.[38] A previous structural study[39] revealed that an H-bond between Lys101 and Glu138 (p51) is disrupted by the Glu138Lys mutation. In our current structure of the wild-type RT:**7** complex, Glu138 also forms a hydrogen bond with Lys101 (Figure 2b).

To examine whether the loss of the H-bond between Lys101 and Glu138 is a primary cause of resistance, we examined the potency of TSAO compounds against mutant HIV-1 strains containing Lys101Glu + Glu138Lys mutations, assuming that switching the positions would retain the 101−138 H-bond. However, the double mutant showed significant resistance (>50-fold) to the TSAO compounds **7** and **8** (Figure 3a; Table 3), suggesting that Glu/Asp is an absolute requirement for the inhibition of HIV-1 RT by TSAO. A prior molecular modeling study predicted that the TSAO compounds bind to a channel between the p51 and p66 subunits near Glu138 (p51) but outside the NNIBP.[40] Potentially, the modeled site[40] may be a transient site for TSAO prior to entering the NNIBP. Although the modeled binding of TSAO does not explain the resistance caused by NNIBP mutations, a non-NNIBP mutation site Arg/Lys172 is in close proximity to the modeled TSAO molecule. The Arg/Lys172Ala mutation causes hypersensitivity to TSAO, presumably by providing better passage for this large NNRTI. The engineered mutation Phe160Ser in RT69A, the protein construct used in the current structural study, is located at the base of the long helix containing the amino acid residue 172. Apparently, the Phe160Ser mutation allows larger adaptability for the helix and the surrounding region (like the helix containing Tyr115 and Phe116), which thereby may provide better accessibility for TSAO compounds to pass through the channel. The TSAO molecules in the model and in the crystal structure are positioned on either side of Glu138, which suggests that Glu138 plays an important role in the entry of TSAO compounds to the

Table 3. Inhibitory Activity of TSAO-T[14] and TSAO-m^{3}T[14b] against Mutant HIV-1 RTs

	IC_{50}[a] (μg/mL)		
HIV-1 RT	7 (TSAO-T)	8 (TSAO-m^{3}T)	ddGTP
wild-type	1.2 ± 0.14	2.4 ± 1.6	0.11 ± 0.05
K101E	≥100	>100	0.12 ± 0.002
E138K	>100	>100	0.11 ± 0.021
K1001E + E138K	>100	>100	0.14 ± 0.014

[a] 50% Inhibitory concentration, or compound concentration required to inhibit the HIV-1 RT-catalyzed polymerization reaction by 50% using poly rC:dG as the template-primer and [3H]dGTP as the radiolabeled substrate. ddGTP was included as a control NRTI. Data are the mean ± SD of at least two independent experiments.

Table 4. Structure−Activity Relationships of TSAO Compounds[53] [a]

	EC_{50} (μM) in CEM cell cultures		IC_{50} (μM)
compd	HIV-1	HIV-2	HIV-1 RT
TSAO-T (**7**[14])	0.06 ± 0.01	>20	1.2 ± 0.14
TSAO-m3T (**8**[14b])	0.04 ± 0.09	>250	2.4 ± 1.6
9[43]	0.01 ± 0.01	>10	0.56 ± 0.09
10[40]	0.17 ± 0.05	>2	ND
11[40]	0.10 ± 0.01	>10	ND
12[44]	0.05 ± 0.02	>10	ND
13[44]	0.06 ± 0.01	>150	ND
14[45]	0.08 ± 0.0	>7	ND
15[46]	5.3 ± 1.2	>7	ND
16[46]	5.8 ± 1.9	>35	ND
17[15]	0.15 ± 0.16	>2	3.3
18[47]	0.028 ± 0.01	>7	ND

[a] EC_{50} were measured in CEM cells and IC_{50} were measured in an HIV-1 RT enzymatic assay.[53]

NNIBP. Mutation of the neighboring conserved residue Asn136 (p51) also causes resistance to TSAO;[41] like Glu138, Asn136 is located at the p66/p51 dimer interface and deletion of Asn136 is deleterious for the stability of the RT heterodimer.[42] A Cα superposition of RT:**7** and RT:**5**[9] structures showed that the 136−138 loop had deviated the most (~2 Å) compared to other amino acid residues of p51 at the dimer interface. Taking together the crystal structure, molecular model, resistance data, and biochemical analysis, it is reasonable to assume that Glu138 and surrounding residues are involved in the entry of TSAO into the NNIBP.

DISCUSSION AND CONCLUSIONS

Structure−Activity Relationships (SAR) of TSAO. Several TSAO derivatives[43] have been synthesized, primarily by modifying the thymine base and the spiro ring (Figure 3a, Table 4); however, clear SAR could not be established because a structure explaining the binding of TSAO to RT was not available. The current crystal structure helps explain the SAR for the TSAO derivatives. Various R-substitutions at the N-3-position of the thymine ring[43] would be accommodated by the space around the 214−224 loop that is outside the NNIBP. A large R-group (R = $(CH_2)_4CONHCH_3$; compound **9**) marginally enhanced the potency of the TSAO by gaining interaction outside NNIBP. The 3-NH group of **7** in the current structure forms a hydrogen bond (N···O distance 2.9 Å) with a water molecule that is coplanar with the thymine ring (Figure 2b). This interaction with a solvent molecule provides support for accommodating a bulkier R-group at the 3-position of the thymine ring replacing the water molecule. The structure also indicates that a carefully modeled R-group can reach the polymerase active site. Substitutions at the 4-position of the thymine ring (compounds **10**[40] and **11**[40]) marginally decrease the potency of HIV-1 inhibition by TSAO (Table 4). In agreement with the structure-based prediction, TSAO compounds (**12** and **13**)[18,44] containing a purine base substituted for the thymine group, retain the anti-HIV-1 property of TSAO. Also, a planar triazole ring substitution for thymine (compound **14**)[45] that can retain the aromatic stacking with Phe227 retains the anti-HIV-1 activity.

The 3′-spiro ring is buried inside the NNIBP and is also responsible for the only H-bond (O···H−N) and for water-mediated interactions between TSAO and RT (Figure 2b). Substitutions in the spiro ring (compounds **15**[46] and **16**[46]) that alters/removes the above-discussed H-bond and the water-mediated interactions with RT impair the potency of TSAO (Figure 3a, Table 4). In contrast, the removal of the amino group from the spiro ring (compound **17**[15]) causes only ~3-fold reduction in EC_{50}. In the RT:TSAO-T crystal structure, the amino group points toward the Leu100 side chain with a minimum distance >4.5 Å from any protein atom; however, the amino group is involved in a water-mediated H-bond with RT (Figure 2b). This water molecule can be displaced when a $-COCONH_2$ group is attached to the amino group (compound **18**),[47] and the substitution retains the anti-HIV-1 activity of TSAO (Table 4). In summary, several substitutions on the TSAO scaffold could enhance inhibitor:protein interaction; however, the substitutions do not improve HIV-1 inhibition by TSAO compounds (Table 4), perhaps because the binding of TSAO requires significant structural rearrangement of RT, as discussed in the following section.

Clinical isolates from HIV-1 infected patients demonstrate that RT can undergo several mutations while retaining its activity. Different laboratories use different strains of RT for their experiments. In our crystallization experiments, RT69A adopted the **7**-bound conformation of RT. The RT69A construct (1) is active,[4] (2) does not contain mutation of any of its functionally important amino acid residues, and (3) has no noticeable difference in its secondary structure arrangements or folding compared to published RT structures. These structural agreements, and the fact that the structure of RT69A:**7** complex fully explains all SAR and mutation data of TSAO class of inhibitors, clearly and validate demonstrate the binding of TSAO to HIV-1 RT.

Hyperexpansion of NNRTI-Binding Pocket. A swivel motion of the primer grip with respect to the YMDD motif is essential for translocation of the nucleic acid after each nucleotide incorporation.[5] The opening of the primer grip can create a transient hydrophobic pocket that accommodates NNRTIs (Figure 4a). The pocket can accommodate a variety of chemically diverse hydrophobic compounds, and the shape and size of the pocket complement the shape and size of the bound NNRTI. The dynamic characteristics of the primer grip and the opening/closing of the pocket is less well understood. However, a comparison of the positions of the primer grip in different RT:NNRTI structures, based on superposition of the YMDD sheet ($\beta6-\beta10-\beta9$), helps to illustrate the widespread distributions of the conformational states of RT and the primer grip

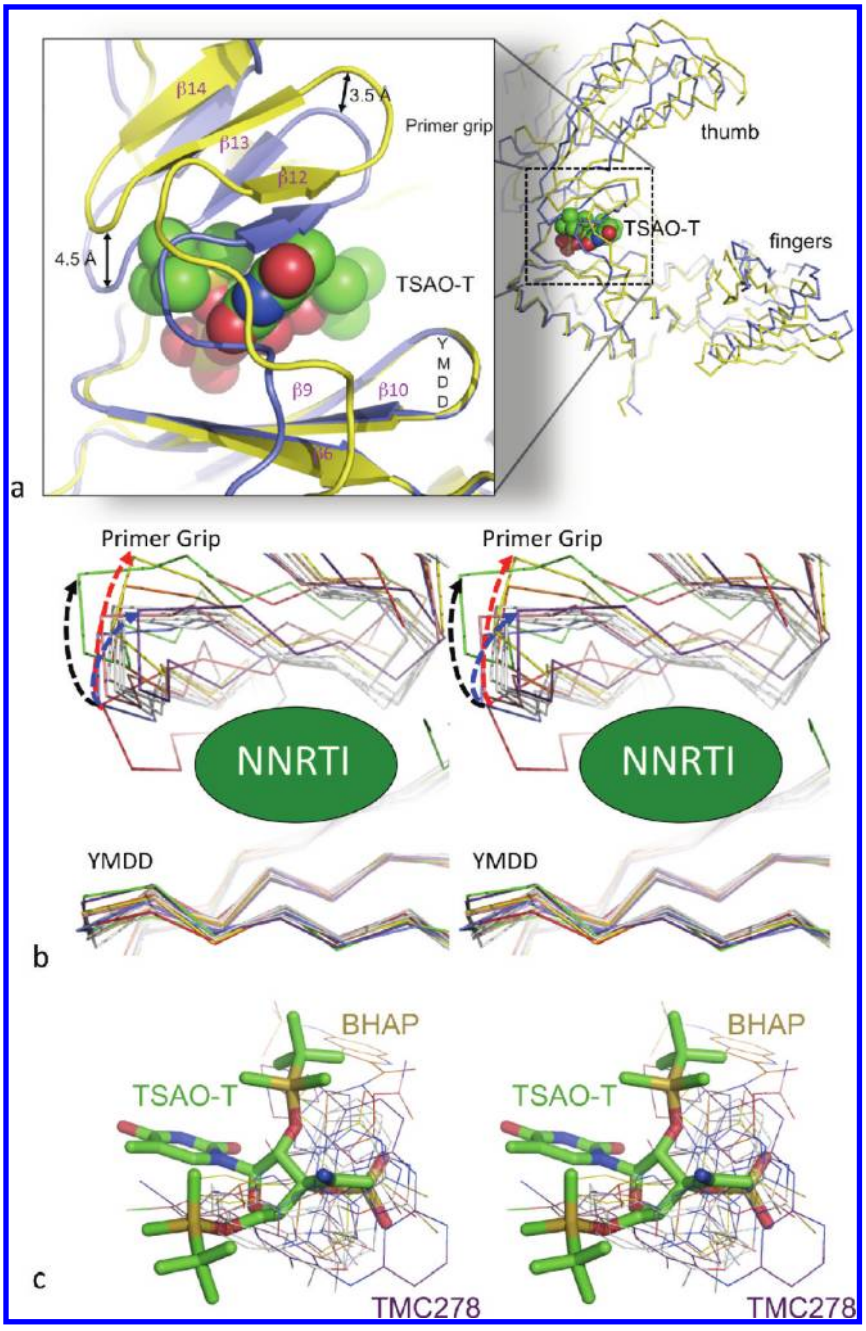

Figure 4. Binding of **7** vs other NNRTIs to HIV-1 RT. (a) The RT conformation is substantially rearranged upon the binding of **7** (TSAO-T in CPK model and RT in yellow) when compared with the **5**-bound conformation of RT (blue). (b) Cluster analysis of the rearrangement of the primer grip with respect to the aligned $\beta6-\beta10-\beta9$ sheet. Upon binding of **7**, the primer grip occupies a distinct position (green) compared to the main cluster[21] and those when **5** (TMC278, purple) and **2** (delavirdine, yellow) are bound. The black, blue, and red arrows indicate the movement of the primer grip from apo RT (red RT), respectively, when **7**, **5**, and **2** are bound. (c) The overlay of NNRTIs using the above superposition of $\beta6-\beta10-\beta9$ sheets of individual RT:NNRTI structures. The NNRTI in (c) and corresponding primer grip in (b) are colored green, purple, and yellow for **7**, **5**, and **2**, respectively.

(Figure 4b). The primer grip positions are clustered when most NNRTI-bound structures were compared; however, the binding of **5**, **2**, and **7** molecules positions the primer grip as outliers, indicating three distinct conformations of the NNIBP. The positioning of **5**, **2**, and **7** in the NNIBP are also different from the common NNRTI cluster and from one another (Figure 4c). As a consequence of the different positioning of NNRTIs in the pocket, the primer grip swings in noticeably different directions with respect to the YMDD motif, as indicated by colored arrows in Figure 4b. This difference in positioning of the primer grip influences the relative positioning of the individual subdomains of RT. For example, the RT:**5** (PDB 2ZD1)[9] and RT:**7** complexes were crystallized in one crystal form with very similar unit cell dimensions, yet the relative positioning of the subdomains are significantly different in the two structures (Figure 4a): the tips of the fingers and thumb subdomains, and the RNase H

dx.doi.org/10.1021/jm101536x |*J. Med. Chem.* 2011, 54, 2727–2737

domains are about 6, 5, and 7 Å apart, respectively, when both the structures were aligned on their β6−β10−β9 sheets.

Effect of TSAO Binding on the RT Dimer. Above analyses revealed that entry of a TSAO inhibitor into the NNIBP requires a significant rearrangement of the β7−β8 loop in the p51subunit, which contains amino acid residues Asn136 and Glu138, known to cause TSAO resistance upon mutation. Alteration of the loop has been shown to disrupt p66/p51 dimerization.[42] In the TSAO-T-bound structure, two β-sheets (β6−β10−β9 and β12−β13−β14) are wide apart, causing a significant long-range distortion of the RT structure (Figure 4). Therefore, it may be assumed that the structural changes required for binding of TSAO to RT, hyperexpansion of NNIBP, and the rearranged conformation of the RT subdomain are predominantly responsible for (1) lower stability of the p66/p51 dimer upon binding of a TSAO compound and (2) the lower potency of TSAO compounds despite their extensive interactions with RT.

Lessons for Drug Design. The crystal structure of RT:7 complex revealed that the NNIBP is surprisingly elastic and flexible and can accommodate very large molecules. However, such unusual expansion of the binding pocket results in a very tight fitting of the large inhibitor in the enzyme, making direct contacts with a wide variety of amino acids lining the ballooned pocket. As a consequence, several TSAO derivatives (Table 4) in which favorable chemical substitutions could increase inhibitor−protein interactions, in fact, did not improve the anti-HIV-1 inhibition of TSAO. Additionally, mutations of NNIBP amino acid residues hardly allow the inhibitor to adapt its conformation or optimal fitting in the enzyme resulting in drug resistance. It seems that both the size of the inhibitor and the expansion of the binding pocket have their limitations for an optimal fitting and adaptation to the amino acid changes. An oversized inhibitor and/or an overexpanded pocket are not advisible for optimal inhibitory activity. These conclusions are in agreement with our findings that (1) the inhibitory activity of the TSAO molecule has never been markedly improved, regardless of the many hundreds of derivatives made from the TSAO prototype molecule and (2) the much smaller and more adaptive DAPY NNRTIs, in contrast, have significantly improved inhibitory activity against wild-type and NNRTI-resistant HIV-1 viruses.[9,31] The RT:7 structure also revealed novel NNRTI design features, such as interactions with the conserved Tyr183 and the opportunity for an NNRTI to reach the polymerase active site, that can be exploited in designing new NNRTIs with smaller scaffolds.

EXPERIMENTAL SECTION

Synthesis of Compounds. TSAO-T (**7**), 2′,5′-bis-*O*-(*tert*-butyldimethylsilyl)-β-D-ribofuranosyl]-3′-spiro-5″-(4″-amino-1″,2″-oxathiole-2″, 2″-dioxide)thymine,[14] TSAO-m^{3}T (**8**), [1-[2′,5′-bis-*O*-(*tert*-butyldimethylsilyl)-β-D-ribofuranosyl]-3-*N*-methylthymine]-3′-spiro-5″-(4″-amino-1″, 2″-oxathiole-2″,2″-dioxide),[14b] compound **9**, [1-[2′,5′-bis-*O*-(*tert*-butyldimethylsilyl)-β-D-ribofuranosyl]-3-*N*-[4-(*N*′-methylcarbamoyl)-butyl]thymine]-3′-spiro-5″-(4″-amino-1″,2″-oxathiole-2″,2″-dioxide),[43] compound **10**, [1-[2′,5′-bis-*O*-(*tert*-butyldimethylsilyl)-β-D-ribofuranosyl]-4-thiothymine]-3′-spiro-5″-(4″-amino-1″,2″-oxathiole-2″,2″-dioxide),[40] compound **11**, [1-[2″,5″-bis-*O*-(*tert*-butyldimethylsilyl)-β-D-ribofuranosyl]-3,4-dihydro-5-methyl-2-pyrimidone]-3′-spiro-5″-(4″-amino-1″, 2″-oxathiole-2″,2″-dioxide),[40] compound **12**, [9-[2′,5′-bis-*O*-(*tert*-butyldimethylsilyl)-β-D-ribofuranosyladenine]-3′-spiro-5″-(4″-amino-1″,2″-oxathiole-2″,2″-dioxide),[44] compound **13**, [9-[2′,5′-bis-*O*-(*tert*-butyldimethylsilyl)-β-D-ribofuranosyl]-1-*N*-methylhypoxanthine]-3′-spiro-5″-(4″-amino-1″,2″-oxathiole-2″,2″-dioxide),[44] compound **14**, [1-[2′,5′-bis-*O*-(*tert*-butyldimethylsilyl)-β-D-ribofuranosyl)]-5-(*N*-methylcarbamoyl)-l,2,3-triazole]-3′-spiro-5″-(4-amino-l″,2″-oxathiole-2,2-dioxide),[45] compound **15**, [1-[2′,5′-bis-*O*-(*tert*-butyldimethylsilyl)-β-D-ribofuranosyl]-3-*N*-methylthymine]-3′-spiro-5″-(4″-amino-1″,2″,3″-oxathiazole-2″, 2″-dioxide),[46] compound **16**, [1-[2′,5′-bis-*O*-(*tert*-butyldimethylsilyl)-β-D-ribofuranosyl]-3-*N*-methylthymine]-3′-spiro-5″-(4″-amino-2″-oxazolone),[46] compound **17**, [1-[2′,5′-bis-O-(*tert*-butyldimethylsilyl)-β-D-ribofuranosyl]-3-*N*-methylthymine]-3′-spiro-5″-(1″,2″-oxathiole-2″, 2″-dioxide),[15] and compound **18**, [1-[2′,5′-bis-*O*-(*tert*-butyldimethylsilyl)-β-D-ribofuranosyl]-3-*N*-(methyl)thymine]-3′-spiro-5″-(4″-oxamoylamino-1″,2″-oxathiole-2″,2″-dioxide),[47] were prepared as previously described. The compounds were >95% pure as determined by HPLC, NMR, and microanalyses.

HIV-1 Reverse Transcriptase Assay. Enzyme reactions (50 μL in volume) were carried out in a 50 mM Tris-HCl (pH 7.8) buffer that contained 5 mM dithiothreitol, 300 mM glutathione, 0.5 mM EDTA, 150 mM KCl, 5 mM $MgCl_2$, 1.25 μg of bovine serum albumin, 0.06% Triton X-100, an appropriate concentration of 2.8 μM [^{3}H]dGTP (2 μCi/assay), varying concentrations of the test compounds, and a fixed concentration of poly(rC)/oligo(dG) (0.1 mM). Reactions were initiated by the addition of 1 μL of wild-type or mutant RT and were incubated for 30 min at 37 °C. Reactions were terminated by the addition of 200 μL of 2 mg/mL yeast RNA, 2 mL of 0.1 M $Na_4P_2O_7$ (in 1 M HCl), and 2 mL of 10% (v/v) trichloroacetic acid. The solutions were kept on ice for 30 min, after which the acid-insoluble material was washed and analyzed for radioactivity.

Expression, Purification, and Crystallization. The protein expression constructs RT69A and RT52A that were tried in crystallizing the RT:7 complex were produced by a previously described crystal engineering process[4] employed to obtain high-resolution structures of HIV-1 RT:NNRTI and apo HIV-1 RT structures, respectively. The proteins were expressed in BL21-CodonPlus-RIL cells, induced with 1 mM IPTG at an OD600 of 0.9, followed by a full expression at 37 °C for 3 h. The samples were purified using a Ni-NTA column (Qiagen, Valencia, CA USA); the eluted samples were treated overnight with HRV14 3C protease (at a ratio of ∼1:100 protease:RT) at 48 °C. The final purification step was carried out using a Mono Q column and the purified RT samples were buffer exchanged and concentrated to 20 mg/mL in 10 mM Tris pH 8.0 and 75 mM NaCl.

The inhibitor was dissolved in dimethyl sulfoxide (DMSO) to a 50 mM stock solution. The RT:7 complexes, in an approximate 1:2 molar ratio, were incubated for 10 min at room temperature prior to crystallization. The hanging-drop vapor diffusion crystallization trays were set up using 9−12% PEG8000, 50 mM imidazole pH 6.8, and 0.1 M ammonium sulfate. Bipyramidal crystals of the RT69A:7 complex were obtained after 7−10 days.

X-Ray Crystallography. The crystals (size ∼0.2 × 0.15 × 0.3 mm^3) were dipped in the well solution containing 25% ethylene glycol and cryocooled in a gaseous N_2 stream at 105° K. X-ray diffraction data from a cryocooled crystal was collected on a Rigaku R-Axis IV^{++} mounted on a rotating anode Cu X-ray source. The data was processed/scaled using HKL2000,[48] and the structure was solved by molecular replacement using the protein atoms of the RT52A:**5** structure[9] as the starting model. Cycles of model building using the graphic software COOT[49] and least-squares refinement using CNS 1.2[50] produced unambiguous difference ($|F_o| - |F_c|$) electron density for **7** (Figure 2a). The software suite PHENIX[51] was used in intermediate stages of the structure refinement. The final structure was refined using CNS 1.2 at 2.6 Å resolution to R and R_{free} of 0.244 and 0.286, respectively (Table 2).

Accession Codes

[†]The coordinates and structure factors for RT:7 (TSAO-T) complex has been deposited with accession code 3QO9.

AUTHOR INFORMATION

Corresponding Author

*For K.D.: phone, 732-235-5634; E-mail, kalyan@cabm.rutgers.edu. For E.A.: phone, 732-235-5323; E-mail, arnold@cabm.rutgers.edu.

ACKNOWLEDGMENT

We acknowledge Ann Stock, Matthew Miller, and the X-ray data collection facility at CABM for help with diffraction data collection. We are grateful to the U.S. National Institutes of Health (NIH; grants R37 MERIT Award AI 27690 to E.A.; R21 Award AI 087201 to K.D.), the KU Leuven (GOA 10/014 to J. B.), the Spanish MICINN (project SAF2009-13914-C02 to M.-J. C.), and the Comunidad de Madrid (project BIPEDD-CM ref S-BIO-0214-2006 to M.-J.C.) for financial support.

ABBREVIATIONS USED

DAPY, diarylpyrimidine; TSAO-T, [2′,5′-bis-*O*-(*tert*-butyldimethylsilyl)-β-D-ribofuranosyl]-3′-spiro-5″-(4″-amino-1″,2″-oxathiole-2″,2″-dioxide)thymine; HIV, human immunodeficiency virus; RT, reverse transcriptase; NNRTI, non-nucleoside RT inhibitor; NNIBP, non-nucleoside inhibitor binding pocket; SAR, structure−activity relationships; TBDMS, *tert*-butyldimethylsilyl

REFERENCES

(1) De Clercq, E. Non-nucleoside reverse transcriptase inhibitors (NNRTIs): past, present, and future. *Chem. Biodiversity* **2004**, *1*, 44–64.

(2) Rodgers, D. W.; Gamblin, S. J.; Harris, B. A.; Ray, S.; Culp, J. S.; Hellmig, B.; Woolf, D. J.; Debouck, C.; Harrison, S. C. The structure of unliganded reverse transcriptase from the human immunodeficiency virus type 1. *Proc. Natl. Acad. Sci. U.S.A.* **1995**, *92*, 1222–1226.

(3) Hsiou, Y.; Ding, J.; Das, K.; Clark, A. D., Jr.; Hughes, S. H.; Arnold, E. Structure of unliganded HIV-1 reverse transcriptase at 2.7 A resolution: implications of conformational changes for polymerization and inhibition mechanisms. *Structure* **1996**, *4*, 853–860.

(4) Bauman, J. D.; Das, K.; Ho, W. C.; Baweja, M.; Himmel, D. M.; Clark, A. D., Jr.; Oren, D. A.; Boyer, P. L.; Hughes, S. H.; Shatkin, A. J.; Arnold, E. Crystal engineering of HIV-1 reverse transcriptase for structure-based drug design. *Nucleic Acids Res.* **2008**, *36*, 5083–5092.

(5) Das, K.; Sarafianos, S. G.; Clark, A. D., Jr.; Boyer, P. L.; Hughes, S. H.; Arnold, E. Crystal structures of clinically relevant Lys103Asn/Tyr181Cys double mutant HIV-1 reverse transcriptase in complexes with ATP and non-nucleoside inhibitor HBY 097. *J. Mol. Biol.* **2007**, *365*, 77–89.

(6) Ludovici, D. W.; De Corte, B. L.; Kukla, M. J.; Ye, H.; Ho, C. Y.; Lichtenstein, M. A.; Kavash, R. W.; Andries, K.; de Bethune, M.; Azijn, H.; Pauwels, R.; Lewi, P. J.; Heeres, J.; Koymans, L. M.; de Jonge, M. R.; Van Aken, K. J.; Daeyaert, F. F.; Das, K.; Arnold, E.; Janssen, P. A. Evolution of anti-HIV drug candidates. Part 3: diarylpyrimidine (DAPY) analogues. *Bioorg. Med. Chem. Lett.* **2001**, *11*, 2235–2239.

(7) Janssen, P. A.; Lewi, P. J.; Arnold, E.; Daeyaert, F.; de Jonge, M.; Heeres, J.; Koymans, L.; Vinkers, M.; Guillemont, J.; Pasquier, E.; Kukla, M.; Ludovici, D.; Andries, K.; de Bethune, M. P.; Pauwels, R.; Das, K.; Clark, A. D., Jr.; Frenkel, Y. V.; Hughes, S. H.; Medaer, B.; De Knaep, F.; Bohets, H.; De Clerck, F.; Lampo, A.; Williams, P.; Stoffels, P. In search of a novel anti-HIV drug: multidisciplinary coordination in the discovery of 4-[[4-[[4-[(1*E*)-2-cyanoethenyl]-2,6-dimethylphenyl]amino]-2-pyrimidinyl]amino]benzonitrile (R278474, rilpivirine). *J. Med. Chem.* **2005**, *48*, 1901–1909.

(8) Das, K.; Lewi, P. J.; Hughes, S. H.; Arnold, E. Crystallography and the design of anti-AIDS drugs: conformational flexibility and positional adaptability are important in the design of non-nucleoside HIV-1 reverse transcriptase inhibitors. *Prog. Biophys. Mol. Biol.* **2005**, *88*, 209–231.

(9) Das, K.; Bauman, J. D.; Clark, A. D., Jr.; Frenkel, Y. V.; Lewi, P. J.; Shatkin, A. J.; Hughes, S. H.; Arnold, E. High-resolution structures of HIV-1 reverse transcriptase/TMC278 complexes: strategic flexibility explains potency against resistance mutations. *Proc. Natl. Acad. Sci. U.S.A.* **2008**, *105*, 1466–1471.

(10) Llibre, J. M.; Santos, J. R.; Puig, T.; Molto, J.; Ruiz, L.; Paredes, R.; Clotet, B. Prevalence of etravirine-associated mutations in clinical samples with resistance to nevirapine and efavirenz. *J. Antimicrob. Chemother.* **2008**, *62*, 909–913.

(11) Menendez-Arias, L. Molecular basis of human immunodeficiency virus drug resistance: an update. *Antiviral Res.* **2010**, *85*, 210–231.

(12) Balzarini, J.; Pérez-Pérez, M. J.; San-Félix, A.; Schols, D.; Perno, C. F.; Vandamme, A. M.; Camarasa, M. J.; De Clercq, E. 2′,5′-Bis-*O*-(*tert*-butyldimethylsilyl)-3′-spiro-5″-(4″-amino-1″,2″-oxathiole-2″,2′-dioxide)pyrimidine (TSAO) nucleoside analogues: highlyselective inhibitors of human immunodeficiency virus type 1 that are targeted at the viral reverse transcriptase. *Proc. Natl. Acad. Sci. U.S.A.* **1992**, *89*, 4392–4396.

(13) Camarasa, M. J.; San-Félix, A.; Velázquez, S.; Pérez-Pérez, M. J.; Gago, F.; Balzarini, J. TSAO compounds: the comprehensive story of a unique family of HIV-1 specific inhibitors of reverse transcriptase. *Curr. Top. Med. Chem.* **2004**, *4*, 945–963.

(14) (a) Camarasa, M. J.; Pérez-Pérez, M. J.; San-Félix, A.; Balzarini, J.; De Clercq, E. 3′-Spiro nucleosides, a new class of specific human immunodeficiency virus type 1 inhibitors: synthesis and antiviral activity of [2′-5′-bis-*O*-(*tert*-butyldimethylsilyl)-beta-D-xylo- and -ribofuranose]-3′-spiro-5″-[4″-amino-1″,2″-oxathiole 2″,2″-dioxide] (TSAO) pyrimidine nucleosides. *J. Med. Chem.* **1992**, *35*, 2721–2727. (b) Pérez-Pérez, M. J.; San-Félix, A.; Balzarini, J.; De Clercq, E.; Camarasa, M. J. TSAO-analogues. Stereospecific synthesis and anti-HIV-1 activity of 1-[2′,5′-bis-*O*-(*tert*-butyldimethylsilyl)-beta-D-ribofuranosyl]-3′-spiro-5″-(4″-amino-1″,2″-oxathiole-2″,2″-dioxide) pyrimidine and pyrimidine-modified nucleosides. *J. Med. Chem.* **1992**, *35*, 2988–2995.

(15) de Castro, S.; García-Aparicio, C.; Van Laethem, K.; Gago, F.; Lobatón, E.; De Clercq, E.; Balzarini, J.; Camarasa, M. J.; Velázquez, S. Discovery of TSAO derivatives with an unusual HIV-1 activity/resistance profile. *Antiviral Res.* **2006**, *71*, 15–23.

(16) Camarasa, M. J.; Velázquez, S.; San-Félix, A.; Pérez-Pérez, M. J.; Bonache, M. C.; De Castro, S. TSAO derivatives, inhibitors of HIV-1 reverse transcriptase dimerization: recent progress. *Curr. Pharm. Des.* **2006**, *12*, 1895–1907.

(17) Balzarini, J.; Pérez-Pérez, M. J.; San-Félix, A.; Camarasa, M. J.; Bathurst, I. C.; Barr, P. J.; De Clercq, E. Kinetics of inhibition of human immunodeficiency virus type 1 (HIV-1) reverse transcriptase by the novel HIV-1-specific nucleoside analogue [2′,5′-bis-*O*-(*tert*-butyldimethylsilyl)-beta-D-ribofuranosyl]-3′-spiro-5″-(4″-amino-1″,2″-oxathiole-2″,2″-dioxide)thymine (TSAO-T). *J. Biol. Chem.* **1992**, *267*, 11831–11838.

(18) Balzarini, J.; Karlsson, A.; Vandamme, A. M.; Pérez-Pérez, M. J.; Zhang, H.; Vrang, L.; Öberg, B.; Bäckbro, K.; Unge, T.; San-Félix, A.; Velázquez, S.; Camarasa, M. J.; De Clercq, E. Human immunodeficiency virus type 1 (HIV-1) strains selected for resistance against the HIV-1-specific [2′,5′-bis-*O*-(*tert*-butyldimethylsilyl)-3′-spiro-5″-(4″-amino-1″,2″-oxathiole-2″,2″-dioxide)]-beta-D-pentofurano syl (TSAO) nucleoside analogues retain sensitivity to HIV-1-specific nonnucleoside inhibitors. *Proc. Natl. Acad. Sci. U.S.A.* **1993**, *90*, 6952–6956.

(19) Balzarini, J.; Karlsson, A.; Pérez-Pérez, M. J.; Vrang, L.; Walbers, J.; Zhang, H.; Öberg, B.; Vandamme, A. M.; Camarasa, M. J.; De Clercq, E. HIV-1-specific reverse transcriptase inhibitors show differential activity against HIV-1 mutant strains containing different amino acid substitutions in the reverse transcriptase. *Virology* **1993**, *192*, 246–253.

(20) Balzarini, J.; Karlsson, A.; Pérez-Pérez, M. J.; Camarasa, M. J.; De Clercq, E. Knocking-out concentrations of HIV-1-specific inhibitors completely suppress HIV-1 infection and prevent the emergence of drug-resistant virus. *Virology* **1993**, *196*, 576–585.

(21) Paris, K. A.; Haq, O.; Felts, A. K.; Das, K.; Arnold, E.; Levy, R. M. Conformational landscape of the human immunodeficiency virus type 1 reverse transcriptase non-nucleoside inhibitor binding pocket: lessons for inhibitor design from a cluster analysis of many crystal structures. *J. Med. Chem.* **2009**, *52*, 6413–6420.

(22) Sluis-Cremer, N.; Dmitrienko, G. I.; Balzarini, J.; Camarasa, M. J.; Parniak, M. A. Human immunodeficiency virus type 1 reverse transcriptase dimer destabilization by 1-[spiro[4″-amino-2″,2″-dioxo-1″,2″-oxathiole-5″,3′-[2′, 5′-bis-*O*-(*tert*-butyldimethylsilyl)-beta-D-ribofuranosyl]]]-3-ethylthymine. *Biochemistry* **2000**, *39*, 1427–1433.

(23) Sluis-Cremer, N.; Hamamouch, N.; San Felix, A.; Velázquez, S.; Balzarini, J.; Camarasa, M. J. Structure−activity relationships of [2′,5′-bis-*O*-(*tert*-butyldimethylsilyl)-beta-D-ribofuranosyl]-3′-spiro-5″-(4″-amino-1″,2″-oxathiole-2″,2″-dioxide)thymine derivatives as inhibitors of HIV-1 reverse transcriptase dimerization. *J. Med. Chem.* **2006**, *49*, 4834–4841.

(24) Tachedjian, G.; Orlova, M.; Sarafianos, S. G.; Arnold, E.; Goff, S. P. Nonnucleoside reverse transcriptase inhibitors are chemical enhancers of dimerization of the HIV type 1 reverse transcriptase. *Proc. Natl. Acad. Sci. U.S.A.* **2001**, *98*, 7188–7193.

(25) Ding, J.; Das, K.; Moereels, H.; Koymans, L.; Andries, K.; Janssen, P. A.; Hughes, S. H.; Arnold, E. Structure of HIV-1 RT/TIBO R 86183 complex reveals similarity in the binding of diverse nonnucleoside inhibitors. *Nature Struct. Biol.* **1995**, *2*, 407–415.

(26) Hopkins, A. L.; Ren, J.; Esnouf, R. M.; Willcox, B. E.; Jones, E. Y.; Ross, C.; Miyasaka, T.; Walker, R. T.; Tanaka, H.; Stammers, D. K.; Stuart, D. I. Complexes of HIV-1 reverse transcriptase with inhibitors of the HEPT series reveal conformational changes relevant to the design of potent non-nucleoside inhibitors. *J. Med. Chem.* **1996**, *39*, 1589–1600.

(27) Himmel, D. M.; Das, K.; Clark, A. D., Jr.; Hughes, S. H.; Benjahad, A.; Oumouch, S.; Guillemont, J.; Coupa, S.; Poncelet, A.; Csoka, I.; Meyer, C.; Andries, K.; Nguyen, C. H.; Grierson, D. S.; Arnold, E. Crystal structures for HIV-1 reverse transcriptase in complexes with three pyridinone derivatives: a new class of non-nucleoside inhibitors effective against a broad range of drug-resistant strains. *J. Med. Chem.* **2005**, *48*, 7582–7591.

(28) Ingate, S.; Pérez-Pérez, M. J.; De Clercq, E.; Balzarini, J.; Camarasa, M. J. Synthesis and anti-HIV-1 activity of novel TSAO-T derivatives modified at the 2′- and 5′-positions of the sugar moiety. *Antiviral Res.* **1995**, *27*, 281–299.

(29) Chamorro, C.; Pérez-Pérez, M. J.; Rodríguez-Barrios, F.; Gago, F.; De Clercq, E.; Balzarini, J.; San-Félix, A.; Camarasa, M. J. Exploiting the role of the 5′-position of TSAO-T. Synthesis and anti-HIV evaluation of novel TSAO-T derivatives. *Antiviral Res.* **2001**, *50*, 207–222.

(30) San-Félix, A.; Chamorro, C.; Pérez-Pérez, M. J.; Velázquez, S.; De Clercq, E.; Balzarini, J.; Camarasa, M. J. Synthesis of novel 5′-substituted TSAO-T analogues with anti-HIV-1 activity. *J. Carbohydr. Chem.* **2000**, *19*, 635–640.

(31) Das, K.; Clark, J., A.D.; Lewi, P. J.; Heeres, J.; de Jonge, M. R.; Koymans, L. M. H.; Vinkers, H. M.; Daeyaert, F.; Ludovici, D. W.; Kukla, M. J.; De Corte, B.; Kavash, R. W.; Ho, C. Y.; Ye, H.; Lichtenstein, M. A.; Andries, K.; Pauwels, R.; de Béthune, M.-P.; Boyer, P. L.; Clark, P.; Hughes, S. H.; Janssen, P. A. J.; Arnold, E. Roles of Conformational and Positional Adaptability in Structure-Based Design of TMC125-R165335 (Etravirine) and Related Non-nucleoside Reverse Transcriptase Inhibitors That Are Highly Potent and Effective against Wild-Type and Drug-Resistant HIV-1 Variants. *J. Med. Chem.* **2004**, *47*, 2550–2560.

(32) Hsiou, Y.; Ding, J.; Das, K.; Clark, A. D., Jr.; Boyer, P. L.; Lewi, P.; Janssen, P. A.; Kleim, J. P.; Rosner, M.; Hughes, S. H.; Arnold, E. The Lys103Asn mutation of HIV-1 RT: a novel mechanism of drug resistance. *J. Mol. Biol.* **2001**, *309*, 437–445.

(33) Ren, J.; Milton, J.; Weaver, K. L.; Short, S. A.; Stuart, D. I.; Stammers, D. K. Structural basis for the resilience of efavirenz (DMP-266) to drug resistance mutations in HIV-1 reverse transcriptase. *Structure* **2000**, *8*, 1089–1094.

(34) Lindberg, J.; Sigurdsson, S.; Löwgren, S.; Andersson, H. O.; Sahlberg, C.; Noréen, R.; Fridborg, K.; Zhang, H.; Unge, T. *Eur. J. Biochem.* **2002**, *269*, 1670–1677.

(35) Udier-Blagović, M.; Tirado-Rives, J.; Jorgensen, W. L. Structural and energetic analyses of the effects of the K103N mutation of HIV-1 reverse transcriptase on efavirenz analogues. *J. Med. Chem.* **2004**, *47*, 2389–2392.

(36) Balzarini, J.; Karlsson, A.; Pérez-Pérez, M. J.; Camarasa, M. J.; Tarpley, W. G.; De Clercq, E. Treatment of human immunodeficiency virus type 1 (HIV-1)-infected cells with combinations of HIV-1-specific inhibitors results in a different resistance pattern than does treatment with single-drug therapy. *J. Virol.* **1993**, *67*, 5353–5359.

(37) Boyer, P. L.; Ding, J.; Arnold, E.; Hughes, S. H. Subunit specificity of mutations that confer resistance to non-nucleoside inhibitors in human immunodeficiency virus type 1 reverse transcriptase. *Antimicrob. Agents Chemother.* **1994**, *38*, 1909–1914.

(38) Pelemans, H.; Aertsen, A.; Van Laethem, K.; Vandamme, A. M.; De Clercq, E.; Pérez-Pérez, M. J.; San-Félix, A.; Velázquez, S.; Camarasa, M. J.; Balzarini, J. Site-directed mutagenesis of human immunodeficiency virus type 1 reverse transcriptase at amino acid position 138. *Virology* **2001**, *280*, 97–106.

(39) Ren, J.; Nichols, C. E.; Stamp, A.; Chamberlain, P. P.; Ferris, R.; Weaver, K. L.; Short, S. A.; Stammers, D. K. Structural insights into mechanisms of non-nucleoside drug resistance for HIV-1 reverse transcriptases mutated at codons 101 or 138. *FEBS J.* **2006**, *273*, 3850–3860.

(40) Rodríguez-Barrios, F.; Pérez, C.; Lobatón, E.; Velázquez, S.; Chamorro, C.; San-Félix, A.; Pérez-Pérez, M. J.; Camarasa, M. J.; Pelemans, H.; Balzarini, J.; Gago, F. Identification of a putative binding site for [2′,5′-bis-*O*-(*tert*-butyldimethylsilyl)-beta-D-ribofuranosyl]-3′-spiro-5″-(4″-amino-1″,2″-oxathiole-2″,2″-dioxide)thymine (TSAO) derivatives at the p51-p66 interface of HIV-1 reverse transcriptase. *J. Med. Chem.* **2001**, *44*, 1853–1865.

(41) Balzarini, J.; Auwerx, J.; Rodríguez-Barrios, F.; Chedad, A.; Farkas, V.; Ceccherini-Silberstein, F.; García-Aparicio, C.; Velázquez, S.; De Clercq, E.; Perno, C. F.; Camarasa, M. J.; Gago, F. The amino acid Asn136 in HIV-1 reverse transcriptase (RT) maintains efficient association of both RT subunits and enables the rational design of novel RT inhibitors. *Mol. Pharmacol.* **2005**, *68*, 49–60.

(42) Upadhyay, A.; Pandey, N.; Mishra, C. A.; Talele, T. T.; Pandey, V. N. A single deletion at position 134, 135, or 136 in the beta 7-beta 8 loop of the p51 subunit of HIV-1 RT disrupts the formation of heterodimeric enzyme. *J. Cell. Biochem.* **2010**, *109*, 598–605.

(43) Bonache, M. C.; Chamorro, C.; Velázquez, S.; De Clercq, E.; Balzarini, J.; Barrios, F. R.; Gago, F.; Camarasa, M. J.; San-Félix, A. Improving the antiviral efficacy and selectivity of HIV-1 reverse transcriptase inhibitor TSAO-T by the introduction of functional groups at the N-3 position. *J. Med. Chem.* **2005**, *48*, 6653–6660.

(44) Velázquez, S.; San-Félix, A.; Pérez-Pérez, M. J.; Balzarini, J.; De Clercq, E.; Camarasa, M. J. TSAO analogues. 3. Synthesis and anti-HIV-1 activity of 2′,5′-bis-*O*-(*tert*-butyldimethylsilyl)-beta-D-ribofuranosyl 3′-spiro-5″-(4″-amino-1″,2″-oxathiole 2″,2″-dioxide) purine and purine-modified nucleosides. *J. Med. Chem.* **1993**, *36*, 3230–3239.

(45) Alvarez, R.; Velázquez, S.; San-Félix, A.; Aquaro, S.; De Clercq, E.; Perno, C. F.; Karlsson, A.; Balzarini, J.; Camarasa, M. J. 1,2,3-Triazole-[2′,5′-bis-*O*-(*tert*-butyldimethylsilyl)-beta-D-ribofuranosyl]-3′-spiro-5″-(4″-amino-1″,2″-oxathiole 2″,2″-dioxide) (TSAO) analogues: synthesis and anti-HIV-1 activity. *J. Med. Chem.* **1994**, *37*, 4185–4194.

(46) (a) Alvarez, R.; Jimeno, M. L.; Pérez-Pérez, M. J.; De Clercq, E.; Balzarini, J.; Camarasa, M. J. Synthesis and anti-human immunodeficiency virus type 1 activity of novel 3′-spiro nucleoside analogues of TSAO-T. *Antivir. Chem. Chemother.* **1997**, *8*, 507–517. (b) Alvarez, R.; Jimeno, M. L.; Gago, F.; Balzarini, J.; Pérez-Pérez, M. J.; Camarasa, M. J. Novel 3′-spiro nucleoside analogues of TSAO-T. Part II. A comparative study based on NMR conformational analysis in solution and theoretical calculations. *Antiviral Chem. Chemother.* **1998**, *9*, 333–340.

(47) de Castro, S.; Lobatón, E.; Pérez-Pérez, M. J.; San-Félix, A.; Cordeiro, A.; Andrei, G.; Snoeck, R.; De Clercq, E.; Balzarini, J.; Camarasa, M. J.; Velázquez, S. Novel [2′,5′-bis-*O*-(*tert*-butyldimethylsilyl)-beta-D-ribofuranosyl]-3′-spiro-5″-(4″-amino-1″,2″-oxathiole-2″,

2′′-dioxide) derivatives with anti-HIV-1 and anti-human-cytomegalovirus activity. *J. Med. Chem.* **2005**, *48*, 1158–1168.

(48) Otwinowski, Z.; Minor, W. DENZO and SCALEPACK. In *Crystallography of Biological Macromolecules*; Rossmann, M. G., Arnold, E., Eds.; Kluwer Academic Publishers: Boston, 2001; Vol. F, pp 226−235.

(49) Emsley, P.; Cowtan, K. Coot: model-building tools for molecular graphics. *Acta Crystallogr., Sect. D: Biol. Crystallogr.* **2004**, *60*, 2126–2132.

(50) Brunger, A. T. Version 1.2 of the Crystallography and NMR system. *Nature Protoc.* **2007**, *2*, 2728–2733.

(51) Adams, P. D.; Afonine, P. V.; Bunkoczi, G.; Chen, V. B.; Davis, I. W.; Echols, N.; Headd, J. J.; Hung, L. W.; Kapral, G. J.; Grosse-Kunstleve, R. W.; McCoy, A. J.; Moriarty, N. W.; Oeffner, R.; Read, R. J.; Richardson, D. C.; Richardson, J. S.; Terwilliger, T. C.; Zwart, P. H. PHENIX: a comprehensive Python-based system for macromolecular structure solution. *Acta Crystallogr., Sect. D: Biol. Crystallogr.* **2010**, *66*, 213–221.

(52) Laskowski, R. A.; MacArthur, M. W.; Thornton, J. M. Evaluation of protein coordinate data sets, in From First Map to Final Model. In *Proceedings of the CCP4 Study Weekend*; Bailey, S., Hubbard, R., Waller, D., Eds.; Daresbury Laboratory: Warrington, UK, 1994; pp 149−159.

(53) Bonache, M. C.; Quesada, E.; Sheen, C. W.; Balzarini, J.; Sluis-Cremer, N.; Pérez-Pérez, M. J.; Camarasa, M. J.; San-Félix, A. Novel N-3 substituted TSAO-T derivatives: synthesis and anti-HIV-evaluation. *Nucleosides, Nucleotides Nucleic Acids* **2008**, *27*, 351–367.